

1 **A NOTE ON STATISTICAL CONSISTENCY OF NUMERICAL**
2 **INTEGRATORS FOR MULTI-SCALE DYNAMICS***

3 JASON FRANK[†] AND GEORG A. GOTTWALD[‡]

4 **Abstract.** A minimal requirement for simulating multi-scale systems is to reproduce the sta-
5 tistical behavior of the slow variables. In particular, a good numerical method should accurately
6 approximate the probability density function of the continuous-time slow variables. In this note we
7 use results from homogenization and from backward error analysis to quantify how errors of time
8 integrators affect the mean behavior of trajectories. We show that numerical simulations converge,
9 not to the exact probability density function (pdf) of the homogenized multi-scale system, but rather
10 to that of the homogenized modified equations following from backward error analysis. Using ho-
11 mogenization theory we find that the observed statistical bias is exacerbated for multi-scale systems
12 driven by fast chaotic dynamics that decorrelate insufficiently rapidly. This suggests that to resolve
13 the statistical behavior of trajectories in certain multi-scale systems solvers of sufficiently high order
14 are necessary. Alternatively, backward error analysis suggests the form of an amended vector field
15 that corrects the lowest order bias in Euler’s method. The resulting scheme, a second order Taylor
16 method, avoids any statistical drift bias. We corroborate our analysis with a numerical example.

17 **Key words.** multi-scale dynamics; homogenization; stochastic parametrization; backward error
18 analysis

19 **AMS subject classifications.** 37Mxx, 65Pxx, 60Gxx

20 **1. Introduction.** When simulating complex multi-scale dynamics one is often
21 interested in the accurate description, not of the full system with all its degrees of
22 freedom, but of only some distinct relevant variables, for example the slow variables.
23 Numerical weather forecasting provides a good example, where we are interested in
24 the dynamics of the large-scale high and low pressure fields which evolve on time scales
25 of days rather than in fast buoyancy oscillations of the atmosphere’s stratification sur-
26 faces. Another example is decadal climate prediction where we are not interested in
27 the actual dynamics of the large-scale atmospheric weather but rather in their effect
28 on the slowly evolving oceanic patterns such as El-Niño. Whereas in the example of
29 numerical weather prediction we desire accurate time evolution of the slow relevant
30 variables, in climate science we are often more interested in statistical properties such
31 as mean global temperature or the frequency of extreme events. Reproducing such
32 mean statistical behavior of the slow variables is a minimal requirement for any simu-
33 lation of complex multi-scale systems. It has long been recognized that the numerical
34 discretization scheme employed to simulate a dynamical system profoundly affects
35 the numerically observed statistical behavior [2, 7, 8]. This note is concerned with
36 the problem of numerically integrating multi-scale systems with the aim to reliably
37 recover their statistical properties.

38
39 We consider here deterministic multi-scale systems of the form

40 (1) $\dot{x} = \frac{1}{\varepsilon} h(x)f_0(y) + f(x, y), \quad x(0) = \xi$

41 (2) $\dot{y} = \frac{1}{\varepsilon^2} g(y), \quad y(0) = \eta,$

*Submitted to the editors DATE.

[†]Mathematical Institute, Utrecht University, P.O. Box 80010, 3508 TA Utrecht, the Netherlands (J.E.Frank@uu.nl).

[‡]School of Mathematics and Statistics, University of Sydney, NSW 2006, Australia, (georg.gottwald@sydney.edu.au).

42 with $x \in \mathbb{R}^d$, $y \in \mathbb{R}^\ell$. The parameter $\varepsilon \ll 1$ characterizes the degree of time scale
 43 separation. Here the slow dynamics evolves on a characteristic time of order 1 and
 44 the fast dynamics on a characteristic time of ε^2 . We assume that the vector fields
 45 $f_0 : \mathbb{R}^\ell \rightarrow \mathbb{R}^m$, $h : \mathbb{R}^d \rightarrow L(\mathbb{R}^d, \mathbb{R}^m)$, $f : \mathbb{R}^d \times \mathbb{R}^\ell \rightarrow \mathbb{R}^d$ and $g : \mathbb{R}^\ell \rightarrow \mathbb{R}^\ell$ satisfy
 46 certain regularity conditions and that the fast y -dynamics is sufficiently chaotic with
 47 compact chaotic attractor $\Lambda \subset \mathbb{R}^\ell$ and ergodic invariant probability measure μ . We
 48 consider the case when $\int_\Lambda f_0 d\mu = 0$, i.e. when classical averaging would yield trivial
 49 constant-in-time dynamics. In this situation the slow dynamics exhibits stochastic
 50 dynamics on the slow time scale $\mathcal{O}(1)$ [12, 33].

51

52 Numerical simulation of the multi-scale system (1)–(2) is challenging: To cap-
 53 ture the slow dynamics of interest, for any fixed value of the time scale separation
 54 parameter ε , we obtain convergence in the limit $\Delta t \rightarrow 0$, but for ε small, the time
 55 step Δt used to propagate the slow variables must be chosen of the order of ε^2 to
 56 resolve the fast dynamics and meet stability restrictions, making direct numerical
 57 simulations computationally impractical. A minimal requirement for a numerical in-
 58 tegrator is that it should reproduce the statistical behavior of the slow variables of
 59 interest. Ideally we would like to employ $\Delta t \sim \mathcal{O}(1)$ ¹. However, we will see that
 60 depending on the statistical behavior of the fast dynamics, in particular on the decay
 61 of the correlation function of $f_0(y)$, a time step $\Delta t \sim \mathcal{O}(\varepsilon^2)$ may not be sufficient
 62 to recover even the statistical behavior of the slow dynamics and one will need time
 63 steps such that $\kappa = \Delta t/\varepsilon^2 \rightarrow 0$ as $\varepsilon \rightarrow 0$. (Note that for $\kappa > 0$ solutions of the
 64 fast integrator do not converge in the limit $\varepsilon \rightarrow 0$ to the exact solution of (2).) In
 65 other words, it is insufficient to simply resolve the fast motions as $\varepsilon \rightarrow 0$, one must
 66 in fact *accurately approximate them* in this limit, even when the goal is to determine
 67 the mean behavior of the slow variables. This inability of numerical time steppers
 68 of order p to reproduce the statistical behavior of the slow dynamics will be linked
 69 to the persistence of $\mathcal{O}(\Delta t^p)$ -terms in the backward error analysis; furthermore these
 70 error terms have a quantifiable influence on the long-time statistics as they will be
 71 shown to correspond to drift corrections in the homogenized diffusive limit equations
 72 of the numerical discrete time maps.

73

74 For multi-scale systems of the form (1)–(2) the statistical behavior of the slow
 75 dynamics, in the limit of infinite time scale separation $\varepsilon \rightarrow 0$, is described by a stochas-
 76 tic differential equation (SDE) which can be explicitly stated. The mathematical tool
 77 to describe the long-time stochastic behavior of slow dynamics is known as *homog-*
 78 *enization* [12, 33]. Homogenization describes the integrated effect of the fast (either
 79 stochastic or chaotic) dynamics on the slow variables as noise. Initially developed for
 80 stochastic multi-scale systems [20, 21, 32], homogenization has been extended recently
 81 to deterministic multi-scale systems. In the deterministic case the theory is restricted
 82 to the skew-product case (1)–(2) in which the slow dynamics does not couple back to
 83 the fast dynamics. The fully coupled case poses the potential problem that the invari-
 84 ant measure of the fast dynamics may not vary smoothly with the slow variable; in
 85 this instance the averaged vector fields may not even be Lipschitz and uniqueness and
 86 existence of the homogenized equation may not be guaranteed. For the deterministic
 87 skew product case (1)–(2), it was shown rigorously that for sufficiently chaotic fast
 88 dynamics the emergent stochastic long-time behavior of the slow dynamics is given
 89 by stochastic differential equations driven by Brownian motion [30, 15, 18]. The as-

¹ Special multi-scale methods have been devised to do this (see, e.g. [9, 10, 11, 19]).

90 sumed mild conditions on the chaoticity of the fast y -dynamics are satisfied by a large
 91 class of maps and flows. For maps, the convergence to Brownian motion holds when
 92 the correlation function is summable. For flows, it suffices that there is a Poincaré
 93 map with these properties (irrespective of the mixing properties of the flow). These
 94 include, but go far beyond, Axiom A diffeomorphisms and flows, Hénon-like attrac-
 95 tors and Lorenz attractors. Precise statements about the validity can be found in
 96 [27, 28, 29]. We remark that for weakly chaotic dynamics when the correlations are
 97 not summable, the noise is not Brownian anymore but rather α -stable [15]². Homog-
 98 enization has been used as a framework for stochastic parametrizations in the context
 99 of numerical weather forecasting and climate science [24, 25, 23, 26, 31, 6, 13] and is
 100 at the core of the design of several efficient numerical multi-scale integrators such as
 101 the heterogeneous multi-scale method [9, 10] and equation-free projection [11, 19].

102
 103 Depending on the underlying deterministic dynamical multi-scale system, the
 104 noise appearing in the limiting homogenized SDE can be either additive or multiplica-
 105 tive. It is well known that the solution of an SDE is sensitive to the approximation of
 106 the Brownian motion. This sensitivity gives rise to the different interpretations of the
 107 noise such as Itô versus Stratonovich interpretations (see the insightful discussion in
 108 [17]). In [15] it was shown that in the case when the slow dynamics is one-dimensional
 109 the stochastic differential equation describing the diffusive behavior of the slow dy-
 110 namics is to be interpreted in the Stratonovich sense. The intuitive argument for this
 111 result is that the noisy SDE is a rough approximation of a smooth dynamical system,
 112 hence in the limiting process of infinite time scale separation classical calculus should
 113 prevail which necessitates the Stratonovich interpretation³. The limiting SDE for de-
 114 terministic discrete-time maps, however, was shown to be neither of Stratonovich nor
 115 of Itô type. The noise is Itô only if the fast dynamics is δ -correlated.

116
 117 This immediately points to a problem when numerically simulating a continuous-
 118 time multi-scale system: The long-term statistics of a dynamical multi-scale system,
 119 be it continuous-time or discrete time, is described by its homogenized limiting SDE.
 120 However, the limiting stochastic differential equation describing the long-time statisti-
 121 cal behavior of the discretized slow dynamics, that is of the numerical integrator,
 122 might be different from that of the continuous-time system it is designed to model.
 123 Using backward error analysis, we show that the leading-order term responsible for
 124 the difference is the limiting second order contribution of the modified equation corre-
 125 sponding to the numerical map. The main contribution of our work is to show that the
 126 local errors of a time stepper generate a long-time error of the mean behavior which
 127 is recovered by homogenization theory. These error terms are of the order $\mathcal{O}(\Delta t^p)$
 128 for a p th order integrator. This result allows us to draw an important practical con-
 129 clusion: In order for a numerical discretization scheme to reproduce the long-time
 130 statistical behavior of the slow dynamics it may be necessary to employ a sufficiently
 131 high order time-stepping method. In particular, the Euler scheme can lead to mas-
 132 sively different statistical behavior with strong bias. This is the case when, as we will
 133 see, the fast chaotic dynamics does not decay sufficiently quickly and its statistical
 134 behavior is far from being close to independent identically distributed (*i.i.d.*) random

²We use the terminology strongly and weakly chaotic here in a manner different from the usual distinction between exponential and algebraic decay of correlations; cf.[14].

³This does not hold for higher-dimensional slow sub-spaces where the noise is neither Stratonovich nor Itô [18] and the conditions for the Wong-Zakai theorem are not satisfied.

135 variables. In contrast, first order schemes *are* sufficient to capture the long-time sta-
 136 tistical behavior for multi-scale systems with chaotic fast dynamics exhibiting rapid
 137 decay of correlation. As we will see, discretization-induced biases can be expressed
 138 using homogenization theory. This allows us to explicitly subtract the bias from the
 139 slow vector field of the deterministic equation (1), resulting in a remarkably accurate
 140 explicit time stepper.

141

142 The paper is organized as follows. In Section 2 we introduce the diffusive limit of
 143 the deterministic multi-scale system (1)–(2) and of its associated Euler scheme. The
 144 diffusive limits of the original continuous-time deterministic multi-scale system and
 145 its Euler discretized version are shown to differ in the drift term. In Section 3 we
 146 present the backward error analysis of Euler’s method and Heun’s method and the
 147 homogenized limit of the lowest order modified equation for each, describing how its
 148 respective long-time statistics differs from that of (1)–(2). Section 4 presents numerical
 149 simulations corroborating our analytical results. We conclude with a summary and
 150 an outlook in Section 5.

151 2. The diffusive limit of the multi-scale system and its Euler scheme.

152 Using fairly weak conditions on the chaoticity of the fast y dynamics, it was recently
 153 proved in [30, 15, 18] that the long-term behavior of deterministic multi-scale sys-
 154 tems (1)–(2) is stochastic and is described on times of order $\mathcal{O}(1)$ by the following
 155 homogenized stochastic differential equation

$$156 \quad (3) \quad dX = F(X) dt + \sigma h(X) \circ dW_t, \quad X(0) = \xi.$$

158 For simplicity of exposition and ease of computation, we choose in the following
 159 $d = m = 1$. The drift term is given by $F(X) = \int_{\Lambda} f(X, y) d\mu$, W_t is unit 1-dimensional
 160 Brownian motion with the variance given by a Green-Kubo formula with

$$161 \quad (4) \quad \frac{1}{2}\sigma^2 = \int_0^{\infty} \mathcal{C}[f_0(y)](t) dt,$$

163 where $\mathcal{C}[f_0(y)](t) = \mathbb{E}[f_0(y)f_0(\varphi^t y)]$ denotes the autocorrelation function of f_0 with
 164 φ^t denoting the flow of the vector field $g(y)$ (in particular, φ^t is independent of ε),
 165 and the expectation

$$166 \quad \mathbb{E}[A] = \int_{\Lambda} A(y) d\mu$$

167 is taken with respect to the fast invariant measure μ . As discussed in the Introduc-
 168 tion, the noise is of Stratonovich type because the smooth dynamical system (1)–(2)
 169 is approximated by a rough SDE (3), and hence classical calculus has to be valid
 170 throughout the limiting procedure of homogenization. For the precise statements we
 171 refer the interested reader to [15].

172

173 When the multi-scale system (1) is discretized with time step Δt by a numerical
 174 integration method, the slow dynamics is given by a map. For instance, the first order
 175 forward Euler method gives

$$176 \quad (5) \quad x_{n+1} = x_n + \Delta t \frac{1}{\varepsilon} h(x_n) f_0(y_n) + \Delta t f(x_n, y_n), \quad x_0 = \xi,$$

178 where $y_n \approx y(n\Delta t)$ is also obtained via a map $y_{n+1} = \Phi(y_n)$ that approximates φ^t on
 179 time Δt . In this paper, we compute $\Phi(y)$ using multiple time stepping, through the

180 K -fold application of the same numerical integrator as used for the slow dynamics,

$$181 \quad (6) \quad y_{n,k+1} = y_{n,k} + \delta t \varepsilon^{-2} g(y_{n,k}), \quad k = 0, \dots, K-1,$$

182 with initial condition $y_{n,0} = y_n$ and time step $\delta t = \Delta t/K^4$. We set $y_{n+1} = y_{n,K}$ to
 183 define the map $y_{n+1} = \Phi(y_n)$. In the limit $\varepsilon \rightarrow 0$ we choose the scaling $\Delta t = \kappa \varepsilon^2$,
 184 where $\kappa > 0$ is a small but finite constant (i.e. we solve the slow equation on the
 185 fast time scale). This implies that the effective stepsize of the fast motion in (6) is
 186 $\delta t \varepsilon^{-2} = \kappa/K$ and the map Φ is independent of ε . Consequently, the fast motion (6)
 187 does not converge in the limit $\varepsilon \rightarrow 0$ to the exact solution of (2). Instead, the constant
 188 K is chosen such that the fast motion is well-resolved for all ε . We also assume that
 189 the discrete dynamics (6) possesses a chaotic attractor that satisfies the conditions
 190 needed for the existence of the SDE limit as discussed below.

191 For the map (5) it was rigorously proven in [15] that the long-time statistics on
 192 times of order $\mathcal{O}(1/\varepsilon^2)$ is governed by the following SDE

$$193 \quad (7) \quad dX = \left(\kappa F(X) - \frac{1}{2} \kappa^2 h(X) h'(X) \mathbb{E}[f_0^2] \right) dt + \kappa \hat{\sigma} h(X) \circ dW_t, \quad X(0) = \xi,$$

195 where $F(X)$ is the same as before for the continuous-time system, W_t is again unit
 196 1-dimensional Brownian motion and the variance is given by a Green-Kubo formula

$$197 \quad (8) \quad \hat{\sigma}^2 = \mathbb{E}[f_0^2] + \sum_{n=1}^{\infty} \mathbb{E}[f_0(\Phi^n y) f_0(y)] + \sum_{n=1}^{\infty} \mathbb{E}[f_0(y) f_0(\Phi^n y)],$$

199 where Φ^n denotes the n -fold application of the discrete map Φ . Evaluating the time
 200 integral in (4) as a Riemann sum, comparison with (8) shows that $\hat{\sigma}^2 \kappa \rightarrow \sigma^2$ for
 201 $\kappa \rightarrow 0$. We remark that for non-zero κ the diffusion coefficient $\hat{\sigma}^2$ may differ from the
 202 diffusion coefficient σ^2 of the continuous system. Rescaling time to be measured in
 203 units of the discretization “time step” κ , (7) can be rewritten as

$$204 \quad (9) \quad dX = \left(F(X) - \frac{1}{2} \kappa h(X) h'(X) \mathbb{E}[f_0^2] \right) dt + \sqrt{\kappa} \hat{\sigma} h(X) \circ dW_t, \quad X(0) = \xi,$$

206 where W_t is unit 1-dimensional Brownian motion on the rescaled time.

207 Comparing the limiting SDE of the discretized map (9) and the limiting SDE for
 208 its associated continuous-time system (3), we see that they differ by an extra drift
 209 term in (9)

$$210 \quad (10) \quad E = -\frac{1}{2} \kappa h(X) h'(X) \mathbb{E}[f_0^2].$$

212 Note that the additional drift term prohibits a Stratonovich interpretation of the noise
 213 and hence for finite Δt the statistics of the map is different from the statistics of the
 214 original continuous-time system (1)–(2), which we identify with the diffusive limit
 215 system (3). A discrepancy of this form was noted in [15] in the case of general maps
 216 where the time step Δt (or rescaled time step κ) was implied. In the case where the
 217 fast dynamics of the discrete Euler map (5) is *i.i.d.*, i.e. $\hat{\sigma}^2 = \mathbb{E}[f_0^2]$, the noise in the
 218 limiting SDE of the discretized map (9) is of the Itô type. This can be heuristically
 219 understood by realizing that if the time step $\kappa \gg \tau_{\text{corr}}$ where τ_{corr} is the decorrela-
 220 tion time of the fast continuous-time y -dynamics, the map is already as rough as the

⁴An alternative strategy would be to use one step for the fast system with time step $\delta t = \kappa \varepsilon^2$ followed by one step of the slow system with time step $\Delta t/K$ and repeat this K times [34, 3].

221 discrete approximation of the noise.

222

223 Although the additional drift term (10) is formally of order $\mathcal{O}(\Delta t)$, depending on
 224 the dynamical system under consideration, the extra term E can be large and distort
 225 the statistical behavior leading to a marked difference between the numerically ob-
 226 served statistical behavior of the slow variable X and the statistical behavior of the
 227 slow variable x of the given continuous-time multi-scale system (1)–(2) to be mod-
 228 elled. In Section 4 we provide such an example and show how an Euler discretization
 229 may produce erroneous statistical information. In the next section we develop a rela-
 230 tionship between the extra drift term (10) obtained in homogenization and backward
 231 error analysis. In particular, we will show that the extra drift term (10) generated
 232 by a first order numerical time-stepper is present in the backward error analysis and
 233 would be absent if the dynamics had been integrated with a higher order scheme in-
 234 stead (however, other terms are typically present in this case). This will show how
 235 the first order errors of an Euler-method directly translate into errors of the mean
 236 behavior.

237 **3. Backward error analysis.** In this section we provide a backward error anal-
 238 ysis to explain the presence of the extra term (10) in the homogenized discrete model
 239 (9) compared to the homogenized continuous-time model (3). We will see that the ex-
 240 tra term arises from the use of the forward Euler scheme for constructing the discrete
 241 model (5). Although the extra term (10) is of order $\mathcal{O}(\Delta t)$ and hence disappears in
 242 the small step size limit, we stress that in the context of multi-scale problems one is
 243 often interested in step size regimes that are insensitive to fast dynamics and $\mathcal{O}(1)$
 244 with respect to the slow dynamics.

245 Backward error analysis [16, 22] has been successfully employed to understand
 246 finite time step effects observed in numerical simulations. The truncation error of a
 247 numerical discretization of an ordinary differential equation (ODE) can be expanded
 248 as an asymptotic series in the step size Δt with terms involving successively higher
 249 derivatives of the vector field. In backward error analysis, the terms of the truncated
 250 series are interpreted as a higher order approximation to another, perturbed vector
 251 field.

252 **3.1. Lowest order modified equations.** We consider a generic differential
 253 equation

$$254 \quad (11) \quad \dot{z} = v(z),$$

255 the solution of which is to be approximated using a numerical method.

256 To understand the qualitative behavior of the numerical solution for finite step
 257 size Δt , one constructs a modified vector field as an asymptotic expansion

$$258 \quad (12) \quad \dot{z} = \tilde{v}(z) = v(z) + \Delta t v_1(z) + \Delta t^2 v_2(z) + \dots,$$

259 where the terms v_1, v_2 , etc. are to be determined such that the solution to (12)
 260 matches the expansion of a numerical method applied to (11) to a higher order of ac-
 261 curacy. The continuous-time solutions to the truncated modified differential equation
 262 (12) approximate to higher order the numerical output than do those of the original
 263 differential equation (11), allowing the modified equation to be used to interpret finite
 264 time step effects observed in the numerical time series.

265 The solution to (12) is expanded in a Taylor series about $z(t)$ to give

$$266 \quad (13) \quad z(t + \Delta t) = z(t) + \Delta t \tilde{v} + \frac{\Delta t^2}{2} \tilde{v}' \tilde{v} + \frac{\Delta t^3}{6} [\tilde{v}''(\tilde{v}, \tilde{v}) + \tilde{v}' \tilde{v}' \tilde{v}] + \mathcal{O}(\Delta t^4),$$

267 where all terms on the right are evaluated at $z(t)$, and where \tilde{v}' denotes the Jacobian
 268 matrix of \tilde{v} , \tilde{v}'' denotes its (symmetric) three-tensor of second partial derivatives,
 269 and $\tilde{v}''(\cdot, \cdot)$ denotes the contraction of this tensor with the two vector arguments.
 270 Substituting the expansion (12) into the above and gathering terms of like order
 271 yields
 272

$$273 \quad (14) \quad z(t + \Delta t) = z(t) + \Delta t v + \Delta t^2 \left[v_1 + \frac{1}{2} v' v \right] +$$

$$274 \quad \Delta t^3 \left[v_2 + \frac{1}{2} (v' v_1 + v'_1 v) + \frac{1}{6} (v''(v, v) + v' v' v) \right] + \mathcal{O}(\Delta t^4).$$

275

276 Next, one determines the functions v_1, v_2 , etc. to match the expansion of a numerical
 277 integrator to higher order.

278 Euler's method is given by $z_{n+1} = z_n + \Delta t v(z_n)$. This formula is consistent with
 279 (14) up to terms of $\mathcal{O}(\Delta t^2)$, and is consequently a first order approximation to (11).
 280 However by choosing

$$281 \quad v_1 = -\frac{1}{2} v' v$$

282 in (12), one finds that Euler's method agrees with (14) up to terms of $\mathcal{O}(\Delta t^3)$. Con-
 283 sequently, while Euler's method is a first order approximation of (11), it is a *second*
 284 *order approximation* to the modified differential equation

$$285 \quad (15) \quad \dot{z} = v - \frac{\Delta t}{2} v' v.$$

286

287 This process may be repeated to derive higher order corrections (v_2, v_3 , etc.) in the
 288 modified equation. The asymptotic expansion generally does not converge for fixed
 289 Δt , but may be optimally truncated [16]. Although for general systems there is no
 290 guarantee that the lowest order corrections will have the most significant impact on
 291 the observed statistics, in our numerical experiments this does appear to be the case.

292 Next consider the second order Runge-Kutta method (i.e. Heun's method)

$$293 \quad (16) \quad z_{n+1} = z_n + \frac{\Delta t}{2} [v(z_n) + v(z_n + \Delta t v(z_n))].$$

294

295 Expanding the right-hand side about z_n gives

$$296 \quad z_{n+1} = z_n + \frac{\Delta t}{2} \left[2v(z_n) + \Delta t v'(z_n) v(z_n) + \frac{\Delta t^2}{2} v''(v, v)(z_n) + \mathcal{O}(\Delta t^3) \right].$$

297 By choosing

$$298 \quad v_1 = 0, \quad v_2 = \frac{1}{12} v''(v, v) - \frac{1}{6} v' v' v$$

299 in (12) we make this formula agree with (14) up to terms of $\mathcal{O}(\Delta t^4)$ so the modified
 300 equation associated with the second order Runge-Kutta method (16) is (up to terms
 301 of $\mathcal{O}(\Delta t^2)$)

$$302 \quad (17) \quad \dot{z} = v(z) + \frac{\Delta t^2}{12} (v''(v, v) - 2v' v' v),$$

303

304 and the second order Runge-Kutta method (16) applied to the ODE (11) is a third
 305 order approximation to (17).
 306

307 Note that the modified equation (15) suggests a correction to Euler's method to
 308 eliminate the second order term in (14). Specifically, one can apply Euler's method
 309 to the differential equation with corrected vector field

$$310 \quad \dot{z} = v(z) + \frac{\Delta t}{2} v'(z)v(z).$$

311 Doing so yields the second order Taylor method

$$312 \quad (18) \quad z_{n+1} = z_n + \Delta t v(z_n) + \frac{\Delta t^2}{2} v'(z_n)v(z_n),$$

313 which can be efficiently implemented using a finite difference approximation in the
 314 last term:

$$315 \quad v'(z_n)v(z_n) \approx \frac{1}{\tau} (v(z_n + \tau v(z_n)) - v(z_n)), \quad \tau = \sqrt{\epsilon_m},$$

316 with machine precision ϵ_m . Matching (18) with (14) shows the Taylor method has
 317 modified equation expansion (up to terms of $\mathcal{O}(\Delta t^2)$)

$$318 \quad (19) \quad \dot{z} = v(z) - \frac{\Delta t^2}{6} (v''(v, v) + v'v'v),$$

319 and is hence is a second order scheme for the original ODE (11). This will turn out
 320 to be advantageous for problems of the form considered here.

321 **3.2. Homogenization of modified equations.** In the limit $\varepsilon \rightarrow 0$, the time
 322 step scales as $\Delta t = \kappa \varepsilon^2$, where $\kappa > 0$ is fixed and small. As we will take this limit to
 323 homogenize the modified equation, we use $\kappa = \Delta t/\varepsilon^2$ as our expansion parameter for
 324 the backward error analysis.

325 The modified vector fields v_1, v_2 , etc. each in turn can be expressed as expansions
 326 in ε . Upon homogenization, the lowest order term of $\mathcal{O}(1/\varepsilon)$ contributes to the diffu-
 327 sion and the $\mathcal{O}(1)$ term contributes to the drift. Terms of higher order in ε vanish in
 328 the homogenization limit $\varepsilon \rightarrow 0$.

329 Substituting the vector fields of the deterministic multi-scale system (1)–(2) into
 330 the modified equation for a first order Euler discretization (15) with $z = (x, y)$ we
 331 obtain

$$332 \quad (20) \quad \dot{x} = \frac{1}{\varepsilon} h(x)f_0(y) + f(x, y)$$

$$333 \quad - \frac{\kappa}{2} \left(\frac{1}{\varepsilon} h(x)f'_0(y)\tilde{g}(y) + h(x)h'(x)f_0^2(y) + \partial_y f(x, y)\tilde{g}(y) + \mathcal{O}(\varepsilon) \right) + \mathcal{O}(\kappa^2)$$

$$334 \quad (21) \quad \dot{y} = \frac{1}{\varepsilon^2} \tilde{g}(y), \quad \tilde{g} = g(y) + \frac{\kappa}{2K} g'(y)g(y) + \mathcal{O}((\kappa/K)^2).$$

336 In the remainder of the Section we substitute the vector field $g(y)$ for the vector
 337 field $\tilde{g}(y)$ of the fast modified equation, and similarly substitute φ^t for $\tilde{\varphi}^t$, the flow
 338 of \tilde{g} , which is again independent of ε since κ and K are fixed. This is admissible
 339 if the numerical scheme for the fast dynamics is sufficiently accurate to resolve its
 340 statistical behaviour and in particular, the autocorrelation function; given the relation
 341 $\delta t = \Delta t/K$ and the scaling $\Delta t = \kappa \varepsilon^2$, it is clear that κ/K should be chosen small
 342 enough to accurately approximate autocorrelation functions of the unscaled chaotic
 343 system with vector field $g(y)$, to allow for the substitution of φ^t for $\tilde{\varphi}^t$.

344 We now show that the associated stochastic limit system of the continuous-time
 345 modified equation of the Euler method (15) is the same as that of the discrete Euler

346 discretization (5). The homogenized dynamics, approximating the dynamics of (20)
 347 on time scales of order $\mathcal{O}(1)$, is given up to $\mathcal{O}(\kappa)$ by

$$348 \quad (22) \quad dX = F(X) dt + \sigma h(X) \circ dW_t, \quad X(0) = \xi.$$

350 where $F(X)$ is the expectation with respect to $y \sim \mu$ of the terms of $\mathcal{O}(1)$ in ε in (20).
 351 Noting that $g(y) = \varepsilon^2 \dot{y}$, we observe that the terms $f'_0(y)g(y)$ and $\partial_y f(x, y)g(y)$ in the
 352 slow modified equation (20) can be written as a total derivative (taking x constant
 353 up to terms of $\mathcal{O}(\varepsilon)$ on the homogenization time scale). Consequently, these terms
 354 vanish in expectation as in, for example,

$$355 \quad (23) \quad \mathbb{E} [\partial_y f(X, y)g(y)] = \mathbb{E} \left[\frac{d}{dt} f(X, y(t)) \Big|_{X \text{ fixed}} \right] = 0,$$

356 and we are left with the drift term

$$357 \quad F(X) = \mathbb{E}[f(X, y)] - \frac{\kappa}{2} h(X) h'(X) \mathbb{E}[f_0^2] \\ 358 \quad (24) \quad = \mathbb{E}[f(X, y)] + E.$$

360 The diffusion coefficient is given by

$$361 \quad (25) \quad \frac{1}{2} \sigma^2 = \int_0^\infty \mathbb{E} [f_0(y) f_0(\tilde{\varphi}^t y)] dt \\ 362 \quad + \frac{\kappa}{2} h(X) \int_0^\infty \left(\mathbb{E} \left[f_0(y) \left(\frac{d}{dt} f_0(\tilde{\varphi}^t y) \right) \right] + \mathbb{E} \left[f_0(\tilde{\varphi}^t y) \left(\frac{d}{dt} f_0(y) \right) \right] \right) dt.$$

365 Using ergodicity of the fast dynamics the spatial average in the second integral can
 366 be expressed as a time-average; partial integration then can be used to show that the
 367 second integral sums to zero. The Green-Kubo formula (8) in the limit of $\varepsilon \rightarrow 0$ is
 368 recovered provided we substitute φ^t for $\tilde{\varphi}^t$ in (25), which we argued above is admissible
 369 provided $\kappa/K \ll 1$. Hence in the limit $\varepsilon \rightarrow 0$ we recover the homogenized equation (9)
 370 for the forward Euler map (5), and the long term statistics of the Euler discretization
 371 captures well the statistics of its associated continuous-time modified equation.

372 For a second order method, such as the Runge-Kutta method (16) or second order
 373 Taylor method (18), the additional drift term E is absent from the modified equation.
 374 Nevertheless there are terms of $\mathcal{O}(\kappa^2)$ that could potentially influence the homogenized
 375 limit. When the Runge-Kutta method (16) is applied to the deterministic multi-scale
 376 system (1)–(2), the lowest order modified equation (17) yields, for the slow variable:

$$377 \quad (26) \quad \dot{x} = \frac{1}{\varepsilon} h(x) f_0(y) + f(x, y) \\ 378 \quad + \frac{\kappa^2}{12} \left(\frac{1}{\varepsilon} [h(x) (f''_0(y) g^2(y) - 2f'_0(y) g'(y) g(y))] \right. \\ 379 \quad \left. + [\partial_{yy} f(x, y) g^2(y) - 2\partial_y f(x, y) g'(y) g(y)] + \mathcal{O}(\varepsilon) \right) + \mathcal{O}(\kappa^3).$$

382 The homogenized drift term becomes

$$383 \quad F(X) = \mathbb{E} \left[f(X, y) + \frac{\kappa^2}{12} (\partial_{yy} f(X, y) g^2(y) - 2\partial_y f(X, y) g'(y) g(y)) \right] + \mathcal{O}(\kappa^3),$$

384 which implies an $\mathcal{O}(\kappa^2)$ bias in the drift of the slow variables in the limit $\varepsilon \rightarrow 0$. The
 385 homogenized diffusion parameter becomes

$$386 \quad \frac{1}{2}\sigma^2 = h(X) \int_0^\infty \mathcal{C} \left[f_0(y) + \frac{\kappa^2}{12} (f_0''(y)g^2(y) - 2f_0'(y)g'(y)g(y)) \right] (t) dt + \mathcal{O}(\kappa^3).$$

387 Here, too, an $\mathcal{O}(\kappa^2)$ bias occurs as $\varepsilon \rightarrow 0$.

388 Finally, when the Taylor method (18) is applied to the deterministic multi-scale
 389 system (1)–(2), the lowest order modified equation (19) yields, for the slow variable:

$$390 \quad (27) \quad \dot{x} = \frac{1}{\varepsilon} h(x)f_0(y) + f(x, y) + \frac{\kappa^2}{6} \left(\frac{1}{\varepsilon} v_1^{\text{diff}}(x, y) + v_1^{\text{drift}}(x, y) + \mathcal{O}(\varepsilon) \right) + \mathcal{O}(\kappa^3),$$

391 where

$$392 \quad v_1^{\text{diff}}(x, y) = h(x)f_0''(y)g^2(y) + h(x)f_0'(y)g'(y)g(y),$$

393 and

$$394 \quad v_1^{\text{drift}}(x, y) = 3h(x)'h(x)f_0'(y)f_0(y)g(y) + \partial_{yy}f(x, y)g^2(y) + \partial_y f(x, y)g'(y)g(y).$$

395 Noting that $g(y) = \varepsilon^2 \dot{y}$, we observe that all terms in the drift perturbation can be
 396 written as total derivatives with x fixed and vanish in expectation (cf. (23)):

$$397 \quad \mathbb{E}[v_1^{\text{drift}}(X, y)] = \mathbb{E} \left[3h'(X)h(X) \frac{d}{dt} \left(\frac{f_0^2(y)}{2} \right) + \frac{d}{dt} (\partial_y f(X, y)g(y))_{X \text{ fixed}} \right] = 0.$$

398 Consequently, the Taylor method has *no bias in drift* to $\mathcal{O}(\Delta t^3)$, and we expect the
 399 drift to be simply given by

$$400 \quad (28) \quad F(X) = \mathbb{E}[f(X, y)].$$

401 The diffusion term is also a total derivative:

$$402 \quad v_1^{\text{diff}}(x, y) = \frac{1}{\varepsilon} h(X) \frac{d}{dt} (f_0'(y)g(y)),$$

403 and the diffusion parameter σ is of the form

$$404 \quad \frac{1}{2}\sigma^2 = h(X) \int_0^\infty \left(\mathcal{C}[f_0](t) - \frac{\kappa^2}{3} \mathcal{C} \left[\frac{d}{dt} f_0 \right] (t) \right) dt + \mathcal{O}(\kappa^3).$$

405 The term does not vanish; this is a correlation function, not just an expectation.

406 In summary, we note that the additional drift term E of order $\mathcal{O}(\kappa)$ in (24)
 407 is absent in the modified equation of a numerical method which is at least second
 408 order, such as the Runge-Kutta method (16) or the second order Taylor method
 409 (18). For a second order time-stepping method the homogenized modified equation
 410 therefore agrees with the homogenized equation of the full multi-scale system (3)
 411 up to $\mathcal{O}(\kappa^2)$. However, a second order scheme will generally also have additional
 412 corrections to the drift and diffusion which might be of the same magnitude for finite κ
 413 as those corresponding to the continuous-time multi-scale system under consideration.
 414 Remarkably, the second order Taylor method (18) does not have bias of $\mathcal{O}(\kappa^2)$ in the
 415 drift. This can be traced to the fact that the scheme exactly agrees with the second
 416 order Taylor expansion of the error, and consequently its higher order terms are exact
 417 differentials.

418 **4. Numerical demonstration.** We now demonstrate that the additional terms
 419 in the backward error analysis may lead to significant bias in the probability density
 420 estimation for both the first order forward Euler scheme and, to a lesser degree, the
 421 second order Heun's method. In particular we show that the numerical methods
 422 converge for $\varepsilon \rightarrow 0$ with $\Delta t = \kappa \varepsilon^2$ to the homogenized limits of their respective
 423 modified equations, which are different from the long-time statistical limit of the
 424 original deterministic multi-scale system.

425 We consider the deterministic multi-scale system (1)–(2) with

$$426 \quad f_0(y) = ay, \quad h(x) = \sqrt{x}, \quad f(x, y) = b(c - x)y^2,$$

427 so the slow dynamics is described by the continuous-time system

$$428 \quad (29) \quad \dot{x} = \frac{1}{\varepsilon} a \sqrt{x} y + b(c - x)y^2.$$

430 We choose here $a = 0.1$, $b = 0.005$ and $c = 0.75$. The slow dynamics is driven by
 431 $y = \zeta_2 + \zeta_3$ generated by a fast chaotic Rössler system

$$432 \quad (30) \quad \varepsilon^2 \dot{\zeta}_1 = -\zeta_2 - \zeta_3,$$

$$433 \quad (31) \quad \varepsilon^2 \dot{\zeta}_2 = \zeta_1 + r\zeta_2,$$

$$434 \quad (32) \quad \varepsilon^2 \dot{\zeta}_3 = s + (\zeta_1 - u)\zeta_3,$$

436 with $r = s = 0.25$ and $u = 7$. We will compare the results of a numerical integration
 437 of this deterministic multi-scale system using first and second order discretization
 438 methods to results from the associated limiting homogenized SDE of this system,
 439 describing the long-time statistical behavior.

440 The diffusive limiting equation of the multi-scale dynamical system (29)–(32) can be
 441 obtained via the homogenization techniques presented in Section 2 and is given by
 442 the Cox-Ingersoll-Ross (CIR) model [4, 5]

$$443 \quad (33) \quad dX = \sigma a \sqrt{X} dW_t + 2ab(\beta - X) dt,$$

445 where W_t is unit 1-dimensional Brownian motion. The parameters are:

$$446 \quad (34) \quad \alpha = \frac{1}{2} \mathbb{E}[y^2],$$

$$447 \quad (35) \quad \sigma^2 = 2 \int_0^\infty \mathbb{E}[(\varphi^t y)] dt,$$

$$448 \quad (36) \quad \beta = c + \frac{\sigma^2 a^2}{8ab}.$$

450 To approximate α , an ensemble simulation of the (unscaled) Rössler system was car-
 451 ried out using a 1000-member ensemble on a time interval $t \in [0, 3.2 \times 10^4]$ with initial
 452 conditions drawn approximately from μ (see below). We obtain $\alpha = 28.4 \pm 0.1$. To
 453 estimate σ^2 we solve $w_{n+1} = w_n + \varepsilon \Delta t y_n$ where $\Delta t = \kappa \varepsilon^2$ and $\kappa = 0.5$. Then for
 454 a time series of length $N = \lfloor 1/\varepsilon^2 \rfloor$, $w_N \sim \frac{\Delta t}{\sqrt{N}} \sum_{j=1}^{N-1} y_j$ is approximate Brownian
 455 motion with variance $\mathbb{V}[w_N] = \sigma^2 N \Delta t$. In this way the diffusivity is estimated as
 456 $\sigma^2 \approx 0.140 \pm 0.002$.

457 The Cox-Ingersoll-Ross (CIR) model (33) has the closed form solution

$$458 \quad (37) \quad \frac{X(t)}{c(t)} \sim H(t), \quad c(t) = \frac{\sigma^2 a^2}{8ab} (1 - e^{-2\alpha bt}),$$

459

460 where $H(t)$ is a noncentral χ -squared distribution with $8\alpha\beta b/(a^2\sigma^2)$ degrees of free-
 461 dom and noncentrality parameter $c(t)^{-1}e^{-2abt}X(0)$.

462

463 To numerically integrate the two-scale system (29)–(32) we use a multiple time-
 464 stepping approach [22], with a step size $\Delta t = \kappa \varepsilon^2$ for (29) and step size $\delta t = \Delta t/K$
 465 for the fast subsystem (30)–(32). For our illustration we choose successively $\varepsilon \in$
 466 $\{0.05, 0.025, 0.0125, 0.00625\}$ and integrate over the interval $t \in [0, 2.5]$ using $\kappa = 0.5$
 467 and $K = 50$. For this scaling of time step the fast dynamics (30)–(32) is well resolved
 468 but is not solved with increasing accuracy in the limit $\varepsilon \rightarrow 0$. The probability density
 469 function (pdf) of $x(t)$ is estimated using an ensemble with 160000 members. Each
 470 member starts from $x(0) = 1$ but observes a distinct time series $y(t)$. Each member
 471 initial condition $y(0)$ is drawn from the invariant measure μ by letting a randomly
 472 drawn initial condition relax onto the attractor over a transient time of length 25.
 473 We initially compare two different numerical discretizations of the multi-scale system
 474 (29)–(32). Applied to the generic differential equation

475

$$\dot{x}(t) = v(x(t), y(t)),$$

476 these methods are: the forward Euler method

477 (38)

$$x_{n+1} = x_n + \Delta t v(x_n, y_n),$$

478 and the second order Runge-Kutta method (Heun's method)

479 (39)

$$x_{n+1} = x_n + \frac{\Delta t}{2} [v(x_n, y_n) + v(x_n + \Delta t v(x_n, y_n), y_{n+1})].$$

480 In the above equations y_n denotes the approximation to $y(t_n)$ obtained from nK steps
 481 of size δt .

482 When the slow dynamics (29) is discretized using a forward Euler method (38) with
 483 time step Δt we obtain the map

484 (40)
485

$$x_{n+1} = x_n + \Delta t \frac{1}{\varepsilon} a \sqrt{x_n} y_n + \Delta t b (c - x_n) y_n^2.$$

486 We compare the following probability density functions at time $t = 2.5$:

- 487 • [MS1] The empirical pdf of the multi-scale system (29)–(32) computed using
 488 the forward Euler scheme (38).
- 489 • [MS2] The empirical pdf of the multi-scale system (29)–(32) computed using
 490 the second order Runge-Kutta scheme (39).
- 491 • [HMC] The exact pdf (37) of the limiting homogenized stochastic CIR model
 492 (33) with parameters α given by (34) and σ and β given by (35)–(36) associ-
 493 ated with the continuous-time model (29)–(32).

494 Empirical pdfs of the slow variable x are computed using Matlab's histogram counter
 495 with bin size $\Delta x = 0.005$.

496 The rigorous homogenization results presented in Section 2 assert that the long-
 497 time statistics of the full deterministic multi-scale system is described by the pdf
 498 [HMC]. Figure 1 shows convergence of the empirical pdfs of the numerically ap-
 499 proximated multi-scale system, obtained with the forward Euler ([MS1], left frame)
 500 and Runge-Kutta ([MS2], right frame) methods for decreasing ε (dashed lines, with

501 $\varepsilon = 0.05$ in blue, $\varepsilon = 0.025$ in red, $\varepsilon = 0.0125$ in yellow, and $\varepsilon = 0.00625$ in purple). The exact pdf [HMC] is also indicated in each frame (solid black line). Both
 502 numerically computed pdfs appear to converge, in the limit $\varepsilon \rightarrow 0$, $\Delta t = \kappa \varepsilon^2$, to a
 503 density with the wrong mean. The pdf [MS2] of the RK method is significantly closer
 504 to [HMC] than is [MS1], but bias is nevertheless clearly present.
 505

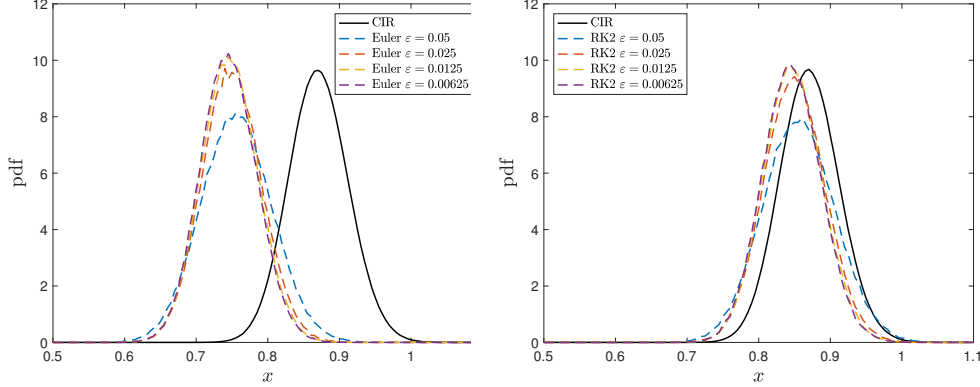


FIG. 1. Comparison of the pdfs of the numerically approximated multi-scale system (29)–(32) with the exact density of the CIR model (37) at time $t = 2.5$ for the forward Euler scheme (38) (left) and the second order Runge-Kutta scheme (39) (right). In each plot the solid black line indicates the exact pdf associated with the homogenized CIR model (33) for the actual time-continuous multi-scale system (29)–(32) (i.e. with parameters (34)–(36)). The dashed lines indicate the empirical probability density function for the numerical simulations of the continuous-time multi-scale system (29)–(32) for $\varepsilon = 0.05$ (blue), 0.025 (red), 0.0125 (yellow), and 0.00625 (purple).

506 For the first order forward Euler discretization (40) the homogenized SDE (22)
 507 describing the long-time behavior of the slow motion is also given by the CIR model
 508 (33), but now with parameters

$$509 \quad (41) \quad \alpha = \frac{1}{2} \mathbb{E}[y^2],$$

$$510 \quad (42) \quad \hat{\sigma}^2 = \mathbb{E}[y^2] + 2 \sum_{n=1}^{\infty} \mathbb{E}[(\Phi^n y)y] = \lim_{n \rightarrow \infty} n^{-1} \mathbb{E}[(\sum_{j=0}^{n-1} \Phi^j y)^2],$$

$$511 \quad (43) \quad \beta = c + \frac{\hat{\sigma}^2 \Delta t a^2}{8\alpha b} - \frac{\Delta t a^2}{4b},$$

513 and $\hat{\sigma}^2 \Delta t \approx \sigma^2$. Note that the only difference in the homogenized CIR systems
 514 associated with the continuous-time multi-scale system (1)–(2) and the discrete Euler
 515 map (40) is in the parameter β (cf. (36) and (43)). For $a^2/b \gg 1$ and $\sigma^2/4\alpha \ll 1$ this
 516 difference is large and may cause significant discrepancy between the statistics of the
 517 continuous-time multi-scale system (29)–(32) and its first order Euler discretization
 518 (40). The latter condition, $\sigma^2/4\alpha = \int_0^\infty \mathbb{E}[(\varphi^t y)y] dt / \mathbb{E}[y^2] \ll 1$ puts a requirement
 519 on the decay of the fast dynamics and states that the fast dynamics should be far
 520 from *i.i.d.* with $\sigma^2 = 2 \mathbb{E}[y^2]$. This requirement is satisfied for the Rössler system
 521 (30)–(32) with the parameters $r = s = 0.25$ and $u = 7$. For these parameters the
 522 autocorrelation function has a slow decay and $\mathbb{E}[y^2] \gg \sigma^2/2$. For comparison, we
 523 introduce an additional pdf:

- 524 • [HMD] The exact pdf (37) of the limiting homogenized stochastic CIR model
- 525 (33) with parameters α given by (34) and σ and β given by (42)–(43) associ-
- 526 ated with the discrete Euler model (40).

527 The backward error analysis presented in Section 3 predicts that the empirical pdf
 528 [MS1] of the Euler method may be better approximated by the pdf [HMD], derived
 529 by homogenizing the modified equation of the Euler method. Figure 2 confirms this
 530 prediction, showing that as $\varepsilon \rightarrow 0$, the statistical behavior of the discrete Euler scheme
 531 is well described by the pdf of its associated homogenized stochastic CIR model. The
 532 extra drift term E in the homogenized discrete model leads to an error of 16% in the
 533 mean of the pdf [HMD] with respect to the mean of the pdf of the original continuous
 534 time multi-scale system (29)–(32) to be modelled [HMC].

535 We remark that for fast chaotic dynamics with rapidly decaying autocorrelation
 536 function such as the Lorenz 63 system with the classical parameters, we have $\mathbb{E}[y^2] \approx$
 537 $\sigma^2/2$. The homogenized equation of the full multi-scale dynamics and its first order
 538 Euler discretization will be close (cf. (36) and (43)), and a first order discretization
 539 would be sufficient to capture the long-time statistics of the slow dynamics.

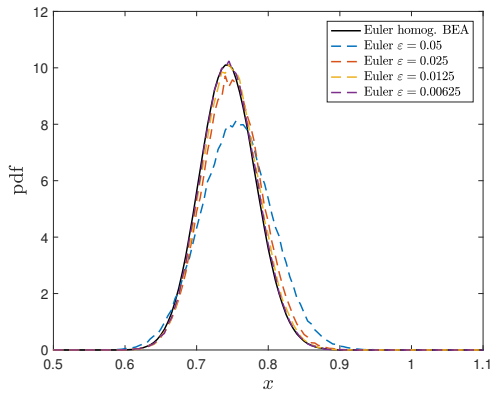


FIG. 2. Comparison of the pdfs of the numerically approximated multi-scale system (29)–(32) with the exact density of the homogenized modified equation model at time $t = 2.5$ for the forward Euler scheme (38). The solid black line indicates the exact pdf associated with the homogenized modified equation (33) of the Euler scheme (i.e. with parameters (41)–(43)). The dashed lines indicate the empirical probability density function computed with the forward Euler approximation (40) applied to the continuous-time multi-scale system (29)–(32) for $\varepsilon = 0.05$ (blue), 0.025 (red), 0.0125 (yellow), and 0.00625 (purple).

540 Finally, the backward error analysis of the second order Taylor method (18) indicates
 541 there is no error in the drift (28) to $\mathcal{O}(\kappa^3)$ for this method. Indeed, Figure 3
 542 confirms this result, illustrating that the empirical pdf of the Taylor method closely
 543 matches that of the pdf [HMC] as $\varepsilon \rightarrow 0$. In fact both the mean and the variance of
 544 the distribution closely match that of the pdf [HMC], suggesting that errors in the
 545 diffusion parameter are also small for this parameter regime. The excellent approxi-
 546 mation of the drift makes the Taylor method an attractive alternative for multi-scale
 547 problems with stochastic limit behavior.

548 **5. Summary.** To summarize, using backward error analysis we have demon-
 549 strated that the extraneous drift term (10) that arises in homogenization of the dis-
 550 crete map (5) compared to homogenization of the flow (1)–(2) can be traced to the
 551 relation between the map (5) and a forward Euler discretization of (1)–(2) with large
 552 step size $\Delta t = 1$. In particular, we relate this drift term which appears in the litera-
 553 ture of homogenization for discrete time systems [15] and which neither corresponds
 554 to an Itô nor to a Stratonovich interpretation of the SDE to discretization errors of
 555 first order schemes using backward error analysis. We have shown that the local first

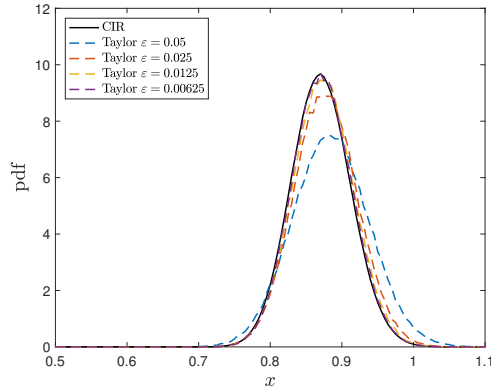


FIG. 3. Comparison of the pdfs of the numerically approximated multi-scale system (29)–(32) with the exact density of the CIR model (37) at time $t = 2.5$ for the second order Taylor method (18). The solid black line indicates the exact pdf associated with the homogenized CIR model (33) for the actual time-continuous multi-scale system (29)–(32) (i.e. with parameters (34)–(36)). The dashed lines indicate the empirical probability density function computed with the second order Taylor method (18) applied to the continuous-time multi-scale system (29)–(32) for $\varepsilon = 0.05$ (blue), 0.025 (red), 0.0125 (yellow), and 0.00625 (purple).

556 order errors contribute to a well-defined drift error, leading to potentially strong bias,
 557 in the long-time statistical behavior. The accumulated local error, as quantified by
 558 the backward error analysis, was shown to account for the long-time statistical error
 559 of the discretization scheme as provided by homogenization theory.

560 We further quantified the requirement for a dynamical system such that its Euler
 561 scheme discretization reliably recovers its long-time statistical behavior. In particular,
 562 we found that for sufficiently rapidly decaying fast dynamics an Euler scheme is suffi-
 563 cient. On the contrary, the failure of first order discretization methods to capture the
 564 statistics of the full continuous-time multi-scale system was shown to be exacerbated if
 565 the fast dynamics exhibits slow decay of correlations. We remark that the slow decay
 566 of correlation is not hampering the validity of the homogenized limit system and the
 567 validity of the underlying functional central limit theorem which is assured solely by
 568 requiring $\varepsilon \ll 1$. The difference is entirely given by the failure to match the limiting
 569 homogenized SDE of the first order discretization with the limiting homogenized SDE
 570 associated with the original time-continuous multi-scale system.

571 Here we discussed deterministic skew product systems of the form (1)–(2). In
 572 order to obtain a stochastic homogenized equation for the slow dynamics, the fast dy-
 573 namics is required to support an ergodic invariant measure and generate an integrable
 574 autocorrelation function of f_0 (cf. the Green-Kubo formula (4)). Hence the conclu-
 575 sions drawn here for the deterministic setting remain valid in the case when the fast
 576 dynamics is stochastic. For a large class of stochastic ordinary differential equations
 577 stochastic integrators were constructed which accurately approximate the invariant
 578 measure [1]. Their construction also uses the framework of modified equations and the
 579 analysis is not restricted to the multi-scale setting. It would be interesting to compare
 580 the higher order methods developed there in the multi-scale setting considered here.
 581 This is a topic for further research.

582

583 In this article, we have examined the limit $\varepsilon \rightarrow 0$, $\Delta t \sim \mathcal{O}(\varepsilon^2)$ in multi-scale
 584 systems (1)–(2) which approach a rigorous SDE limit under homogenization. In this

585 limit, with constant $\kappa = \Delta t/\varepsilon^2 > 0$, the fast motion of the system remains resolved,
 586 but *does not converge* as $\Delta t \rightarrow 0$. The limit is achieved by choosing K to be sufficiently
 587 large and κ/K to be sufficiently small. Our numerical experiments demonstrate sig-
 588 nificant bias in the pdf of the slow variables in the limit $\Delta t \rightarrow 0$ under this scaling.
 589 This bias may be mitigated by reducing the ratio $\kappa = \Delta t/\varepsilon^2$ in the numerical ex-
 590 periments as the bias is multiplied by κ (cf. 10). However, full convergence requires
 591 $\kappa = \Delta t/\varepsilon^2 \rightarrow 0$ as $\varepsilon \rightarrow 0$.

592 We assumed throughout that the fast dynamics is numerically sufficiently resolved
 593 such that the statistical properties, e.g. the auto-correlation structure, is sufficiently
 594 reproduced. If this were not the case, errors arising from the flow map associated with
 595 the fast modified equation enter the Green-Kubo formulae (see, for example, (25) for
 596 the Euler method) implying errors in the diffusion coefficient in addition to the bias
 597 error.

598 We remark that special numerical methods are often specifically tailored to multi-
 599 scale problems to accommodate time steps that are large with respect to the fast time
 600 scale. It is precisely in this regime that statistical bias may occur. The implication
 601 of this for numerical integration of multi-scale systems is that, to avoid statistical
 602 bias, it may be important to use a higher order method for the slow variables. The
 603 second order Taylor method (18) offers an interesting alternative here, as it may be
 604 efficiently implemented and is unbiased with respect to the drift up to $\mathcal{O}(\Delta t^3)$. To
 605 avoid statistical bias altogether, one might want to solve the actual limiting SDE
 606 instead of the deterministic multi-scale system provided that ε is sufficiently small to
 607 allow for the central limit theorem to hold.

608 **Acknowledgments.** We gratefully acknowledge funding through the University
 609 of Sydney – University of Utrecht Partnership Collaboration Award.

610

REFERENCES

- 611 [1] A. ABDULLE, G. VILMART, AND K. C. ZYGALAKIS, *High order numerical approxima-*
 612 *tion of the invariant measure of ergodic sdes*, SIAM Journal on Numerical Analy-
 613 *sis*, 52 (2014), pp. 1600–1622, doi:10.1137/130935616, https://doi.org/10.1137/130935616,
 614 arXiv:https://doi.org/10.1137/130935616.
- 615 [2] R. V. ABRAMOV, G. KOVAČIČ, AND A. J. MAJDA, *Hamiltonian structure and statistically*
 616 *relevant conserved quantities for the truncated burgers-hopf equation*, Communications on
 617 *pure and applied mathematics*, 56 (2003), pp. 1–46.
- 618 [3] G. ARIEL, B. ENGQUIST, S. KIM, Y. LEE, AND R. TSAI, *A multiscale method for highly oscilla-*
 619 *tory dynamical systems using a Poincaré map type technique*, J. Sci. Comput., 54 (2013),
 620 pp. 247–268, doi:10.1007/s10915-012-9656-x.
- 621 [4] J. C. COX, J. E. INGERSOLL, JR., AND S. A. ROSS, *An intertemporal general equilibrium model*
 622 *of asset prices*, Econometrica, 53 (1985), pp. 363–384, doi:10.2307/1911241, http://dx.doi.
 623 org/10.2307/1911241.
- 624 [5] J. C. COX, J. E. INGERSOLL, JR., AND S. A. ROSS, *A theory of the term structure of interest*
 625 *rates*, Econometrica, 53 (1985), pp. 385–407, doi:10.2307/1911242, http://dx.doi.org/10.
 626 2307/1911242.
- 627 [6] J. CULINA, S. KRAVTSOV, AND A. H. MONAHAN, *Stochastic Parameterization Schemes for Use*
 628 *in Realistic Climate Models*, Journal of the Atmospheric Sciences, 68 (2011), pp. 284–299,
 629 doi:10.1175/2010JAS3509.1.
- 630 [7] S. DUBINKINA AND J. FRANK, *Statistical mechanics of Arakawa’s discretizations*, Journal of
 631 *Computational Physics*, 227 (2007), pp. 1286 – 1305.
- 632 [8] S. DUBINKINA AND J. FRANK, *Statistical relevance of vorticity conservation in the Hamiltonian*
 633 *particle-mesh method*, Journal of Computational Physics, 229 (2010), pp. 2634 – 2648.
- 634 [9] W. E, *Analysis of the heterogeneous multiscale method for ordinary differential equations*,
 635 *Comm. Math. Sci.*, 1 (2003), pp. 423–436.
- 636 [10] W. E, B. ENGQUIST, X. LI, W. REN, AND E. VANDEN-ELJNDEN, *Heterogeneous multiscale*
 637 *methods: A review*, Comm. Comp. Phys., 2 (2007), pp. 367–450.

- 638 [11] C. GEAR AND I. KEVREKIDIS, *Projective methods for differential equations*, SIAM J. Sci. Comp.,
639 24 (2003), pp. 1091–1106.
- 640 [12] D. GIVON, R. KUPFERMAN, AND A. STUART, *Extracting macroscopic dynamics: Model problems*
641 *and algorithms*, Nonlinearity, 17 (2004), pp. R55–127.
- 642 [13] G. GOTTWALD, D. CROMMELIN, AND C. FRANZKE, *Ensemble-based Atmospheric Data Assimilation*,
643 in Nonlinear and Stochastic Climate Dynamics, C. L. E. Franzke and T. J. O’Kane,
644 eds., Cambridge University Press, Cambridge, 2017, pp. 209–240.
- 645 [14] G. A. GOTTWALD AND I. MELBOURNE, *A Huygens principle for diffusion and anomalous diffusion*
646 *in spatially extended systems*, Proc. Natl. Acad. Sci. USA, 110 (2013), pp. 8411–8416.
- 647 [15] G. A. GOTTWALD AND I. MELBOURNE, *Homogenization for deterministic maps and multiplicative*
648 *noise*, Proceedings of the Royal Society A: Mathematical, Physical and Engineering
649 Science, 469 (2013).
- 650 [16] E. HAIRER, C. LUBICH, AND G. WANNER, *Geometric numerical integration: structure-*
651 *preserving algorithms for ordinary differential equations*, vol. 31, Springer, 2006.
- 652 [17] W. HORSTHEMKE AND R. LEFEVER, *Noise-induced transitions : theory and applications*
653 *in physics, chemistry, and biology*, Springer series in synergetics, Springer-Verlag, Berlin,
654 New York, 1984, <http://opac.inria.fr/record=b1091778>.
- 655 [18] D. KELLY AND I. MELBOURNE, *Deterministic homogenization for fast–slow systems with chaotic*
656 *noise*, Journal of Functional Analysis, 272 (2017), pp. 4063 – 4102.
- 657 [19] I. G. KEVREKIDIS, C. W. GEAR, J. M. HYMAN, G. K. PANAGIOTIS, O. RUNBORG, AND
658 C. THEODOROPOULOS, *Equation-free, coarse-grained multiscale computation: Enabling*
659 *microscopic simulators to perform system-level analysis*, Comm. Math. Sci., 1 (2003),
660 pp. 715–762.
- 661 [20] R. Z. KHASHMINSKY, *On stochastic processes defined by differential equations with a small pa-*
662 *rameter*, Theory of Probability and its Applications, 11 (1966), pp. 211–228.
- 663 [21] T. G. KURTZ, *A limit theorem for perturbed operator semigroups with applications to random*
664 *evolutions*, Journal of Functional Analysis, 12 (1973), pp. 55–67.
- 665 [22] B. LEIMKUHNER AND S. REICH, *Simulating Hamiltonian Dynamics*, Cambridge University Press,
666 Cambridge, 2005.
- 667 [23] A. MAJDA, I. TIMOFEYEV, AND E. VANDEN-ELJNDEN, *A priori tests of a stochastic mode re-*
668 *duction strategy*, Phys. D, 170 (2002), pp. 206–252, doi:10.1016/S0167-2789(02)00578-X,
669 [http://dx.doi.org/10.1016/S0167-2789\(02\)00578-X](http://dx.doi.org/10.1016/S0167-2789(02)00578-X).
- 670 [24] A. J. MAJDA, I. TIMOFEYEV, AND E. VANDEN ELJNDEN, *Models for stochastic climate prediction*,
671 Proceedings of the National Academy of Sciences, 96 (1999), pp. 14687–14691.
- 672 [25] A. J. MAJDA, I. TIMOFEYEV, AND E. VANDEN ELJNDEN, *A mathematical framework for stochas-*
673 *tic climate models*, Communications on Pure and Applied Mathematics, 54 (2001), pp. 891–
674 974.
- 675 [26] A. J. MAJDA, I. TIMOFEYEV, AND E. VANDEN-ELJNDEN, *Systematic strategies for stochastic*
676 *mode reduction in climate*, Journal of the Atmospheric Sciences, 60 (2003), pp. 1705–1722.
- 677 [27] I. MELBOURNE AND M. NICOL, *Almost sure invariance principle for nonuniformly hyperbolic*
678 *systems*, Commun. Math. Phys., 260 (2005), pp. 131–146.
- 679 [28] I. MELBOURNE AND M. NICOL, *Large deviations for nonuniformly hyperbolic systems*, Trans.
680 Amer. Math. Soc., 360 (2008), pp. 6661–6676, doi:10.1090/S0002-9947-08-04520-0, [http://](http://dx.doi.org/10.1090/S0002-9947-08-04520-0)
681 dx.doi.org/10.1090/S0002-9947-08-04520-0.
- 682 [29] I. MELBOURNE AND M. NICOL, *A vector-valued almost sure invariance principle for hyperbolic*
683 *dynamical systems*, Annals of Probability, 37 (2009), pp. 478–505.
- 684 [30] I. MELBOURNE AND A. STUART, *A note on diffusion limits of chaotic skew-product flows*,
685 Nonlinearity, 24 (2011), pp. 1361–1367.
- 686 [31] A. H. MONAHAN AND J. CULINA, *Stochastic Averaging of Idealized Climate Models*, Journal of
687 Climate, 24 (2011), pp. 3068–3088, doi:10.1175/2011JCLI3641.1.
- 688 [32] G. C. PAPANICOLAOU, *Some probabilistic problems and methods in singular perturbations*,
689 Rocky Mountain Journal of Mathematics, 6 (1976), pp. 653–674.
- 690 [33] G. A. PAVLIOTIS AND A. M. STUART, *Multiscale Methods: Averaging and Homogenization*,
691 Springer, New York, 2008.
- 692 [34] M. TAO, H. OWHADI, AND J. E. MARSDEN, *Nonintrusive and structure preserving multiscale*
693 *integration of stiff ODEs, SDEs, and Hamiltonian systems with hidden slow dynamics via*
694 *flow averaging*, Multiscale Model. Simul., 8 (2010), pp. 1269–1324, doi:10.1137/090771648.